Molecular Catalysis 435 (2017) 1–12

Contents lists available at ScienceDirect

Molecular Catalysis

journal homepage: www.elsevier.com/locate/mcat

MCAT

Editor's choice paper

# Activity of immobilized metallic phthalocyanines in the multicomponent synthesis of dihydropyridine derivatives and their subsequent aromatization

Laura M. Sanchez[a], Ángel G. Sathicq[a], Gustavo P. Romanelli[a], Lina M. González[b], Aida L. Villa[b,*]

[a] Centro de Investigación y Desarrollo en Ciencias Aplicadas "Dr. Jorge J. Ronco" (CINDECA-CCT-CONICET), Universidad Nacional de La Plata, Calle 47 N° 257, B1900AJK La Plata, Argentina
[b] Environmental Catalysis Research Group, Chemical Engineering Department, Engineering Faculty, Universidad de Antioquia UdeA, Calle 70 No. 52-21, Medellín, Colombia

ARTICLE INFO

*Article history:*
Received 14 November 2016
Received in revised form 7 March 2017
Accepted 8 March 2017
Available online 24 March 2017

*Keywords:*
Biomimetic catalyst
Immobilized metallic phthalocyanines
2-Phenylpyridines
Hantzsch reaction
1,4-Dihydropyridines
Multicomponent synthesis

ABSTRACT

Several supported metallo-sulphonated phthalocyanines (FePcS-$NH_2$-$SiO_2$, CoPcS-$NH_2$-$SiO_2$, and CuPcS-$NH_2$-$SiO_2$) and iron hexadecachlorinated phthalocyanines ($FePcCl_{16}$-$NH_2$-$SiO_2$ and $FePcCl_{16}$-$NH_2$-SBA-15) were synthesized and evaluated as alternative catalysts for a green multicomponent Hantzsch reaction between an aromatic aldehyde, methyl or ethylacetoacetate and ammonium acetate to obtain the corresponding dihydropyridines or phenylpyridines depending on the reaction conditions. High selectivities (over 80%) to the 2-phenylpyridines, under oxidant and solvent free conditions at room temperature were obtained. While the formation of 1,4-dihydripyridine derivatives were favored at temperatures above 45 °C (selectivities around of 50%). In addition, the 1,4-dihydripyridine derivatives were aromatized to the corresponding pyridines using *t*-BuOOH as oxidant, acetonitrile as solvent and at a reaction temperature of 50 °C.



## 1. Introduction

The synthesis of nitrogen-heterocyclic compounds, such as dihydropyridines and pyridines, is an interesting area in the development of new drugs. For instance, several 1,4-dihydropyridines (1,4-DHPs) function as neuroprotectants, antianginal [1–3], anti-inflammatory [4], antitubercular [5], analgesic [6] and antithrombotic agents [1,7]. Pyridines could act as potent HIV protease inhibitor [1], and some derivatives are important building blocks for the construction of chemosensors [8].

Hantzsch reaction is one of the most broadly used method for 1,4-DHPs synthesis, and it involves condensation of a β-dicarbonyl compound, **1**, with an aldehyde, **2**, and a source of ammonia (ammonium acetate), **3**; the reaction is typically carried out in acetic acid medium or in refluxing alcohol [9], Fig. 1. It has been reported that asymmetric 2-phenylpyridines could be obtained as the main product, instead of the expected 1,4-DHPs, using the Hantzsch reaction at room temperature, under solvent and oxidant-free conditions and after 72 h of reaction [10].

Notwithstanding, not only temperature but also the presence of a catalyst may change product selectivity; furthermore, after the formation of the ester enamine, **4**, and the Knoevenagel condensation product, **5**, (Fig. 1) the reaction could follow the 1,4 addition through 1,4-dihydropyridine, **6**, with a subsequent oxidation to the corresponding pyridine, **8**, or the 1,2-addition to form the 1,2-dihydropyridine, **7**, with its oxidation to 2-phenylpyridine, **9** [11].

An adequate combination of temperature and acid-base properties of the catalyst has an important role in the selectivity of the Hantzsch reaction [10,11]. Catalytic systems based on $MnO_2$ and $CeO_2$, showed higher selectivity to the 2-phenylpyridine (over 91%) at 25 °C, but the selectivity changed when the temperature was increased to 80 °C, favoring the formation of the 1,4-DHP (75% of selectivity over $CeO_2$) but not the pyridine [11]. Unsupported iron nanoparticles of $Fe_2O_3$ have shown also activity in the synthesis of 1,4-DHPs (yields above 80%) at 90 °C [12].

The use of biomimetic catalysts of the cytochrome P-450 such as phthalocyanines is a topic of interest in the research field, due to the great versatility and reactivity of these molecules which depends on the metal center, the structural changes in the macrocycle, and the substituents present in the periphery, Fig. 2 [13,14]. The phthalocyanines (Pc) have been successfully used in several

* Corresponding author.
*E-mail address:* aida.villa@udea.edu.co (A.L. Villa).

http://dx.doi.org/10.1016/j.mcat.2017.03.010
2468-8231/

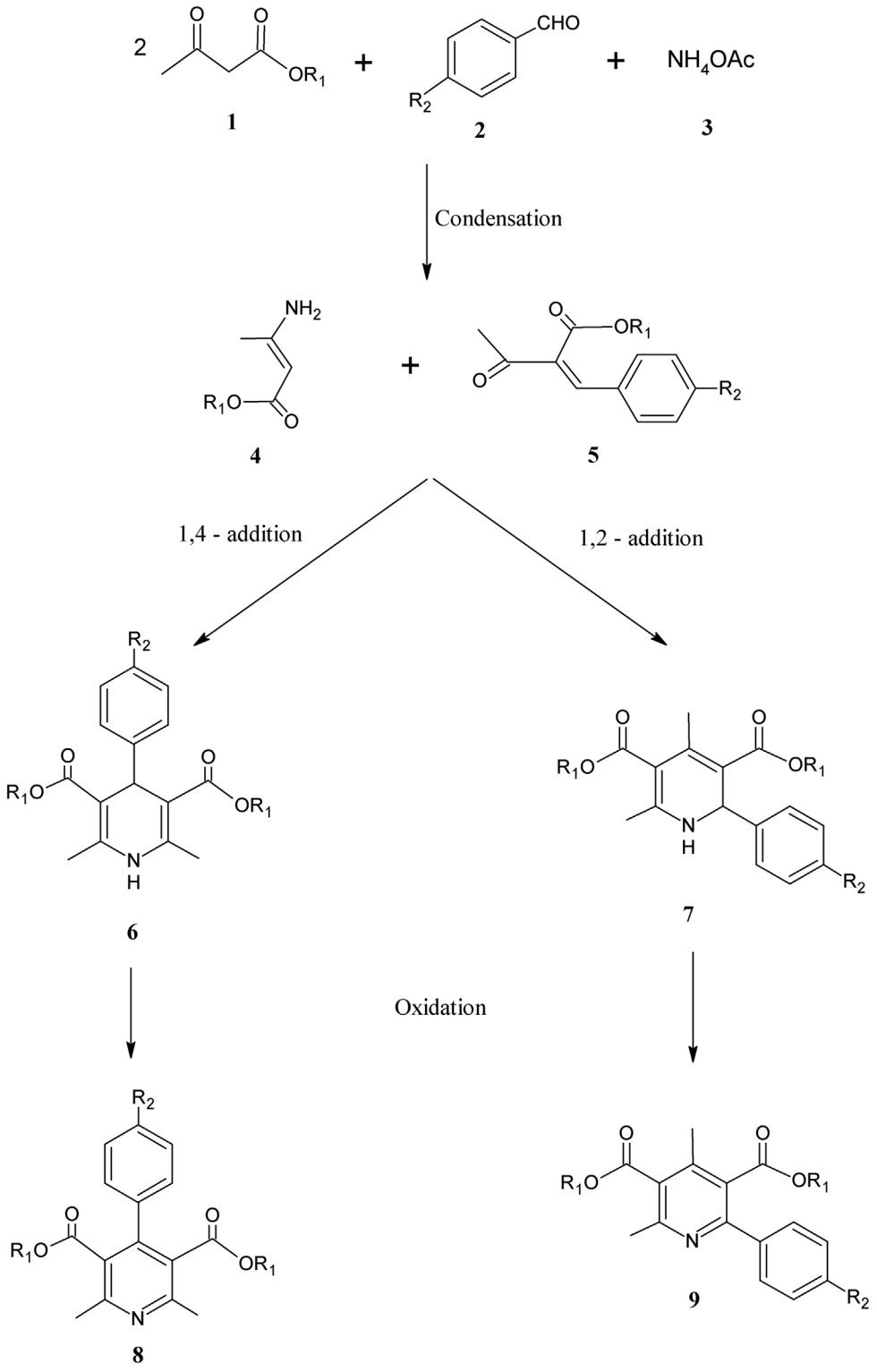


**Fig. 1.** Schematic representation of the synthesis of 1,4- and 1,2-phenylpyridines (compounds **6** and **7**, respectively) and their corresponding oxidation products (compounds **8** and **9**, respectively) over immobilized metallic phthalocyanines as catalysts.

reactions among them oxidations and reductions [14,15], amination and amidation of C—H bonds [16], aziridination of olefins [17], Biginelli condensation to 3,4-dihydropyridinones [18], and C—C coupling [19]. The Pc are very attractive as catalysts due to their low cost and straightforward preparation on a large scale as well as their chemical and thermal stability [20].

Moreover, activity and stability of phthalocyanines can be reached by ring substitution with electron-withdrawing groups, by introduction of a metal to their structure and by their immobilization [14,21,22]. When metal phthalocyanine complexes are immobilized on inorganic supports such as siliceous materials, not only is facilitated their recovery from the reaction media, but also lead to the presence of monomeric and μ-oxo dimeric species

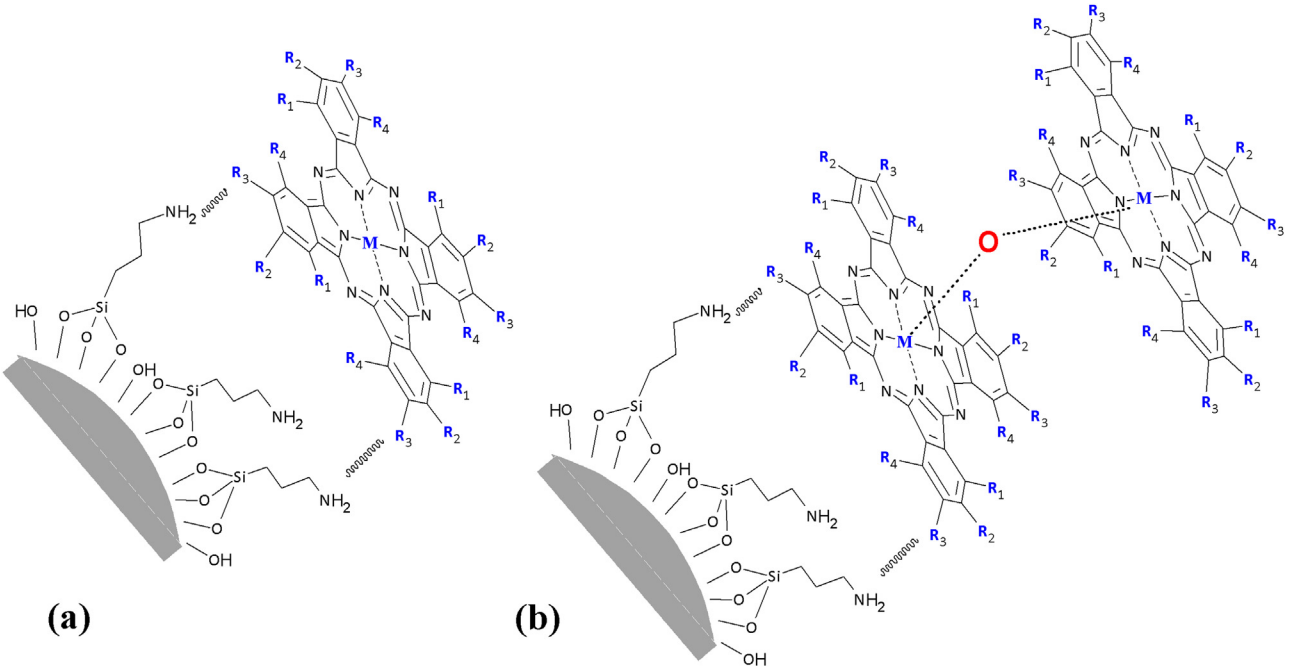


**Fig. 2.** Schematic representation of substituted phthalocyanine MPc supported on $NH_2$-modified support in: a) monomeric or b) μ-oxo dimeric form. M: Center metal, $R_n$: peripheral groups.

with a specific catalytic activity, Fig. 2 [20]. In addition, the use of ordered mesoporous silica SBA-15 is a good alternative for supporting organic complexes, due to the large pore volume and well defined hexagonal arrays of channels and cavities that can improve catalyst activity and selectivity [23,24].

The present research attempts to be in line with the current trend of modify original methods for heterocycles preparation to achieve good yield and selectivity values through the use of greener procedures [25–31]. For example, in replacement of traditional inorganic oxidants commonly used in stoichiometric quantities for dihydropyridine dehydrogenation or aromatization reactions of 1,4-DHPs, some environmentally compatible oxidative agents have been used for these reactions, such as $H_2O_2$ [32], *t*-BuOOH [33] and $CO(NH_2)_2{\cdot}H_2O_2$ [34], among others. A biomimetic oxidation of substituted 1,4-DHPs employing the catalytic system iron(III)-phthalocyanine chloride/*t*-BuOOH and with acetic acid as solvent has been reported with product yields over 88% [14].

In this work we present a novel alternative for nitrogenated heterocyclic compounds synthesis, Fig. 1, over metal-substituted phthalocyanines immobilized on amorphous silica and SBA-15 supports as catalysts. A variety of 2-phenylpyridine derivatives, **7**, were synthesized with the typical reactants and concentrations employed in the Hantzsch reaction. The performance of the heterogeneous catalyst FePcS-$NH_2$-$SiO_2$ was evaluated in the reaction of benzaldehyde, methyl acetoacetate, *t*-BuOOH and ammonium acetate at different temperatures and in the aromatization of 1,4-DHPs under mild and clean conditions, using acetonitrile as solvent and *t*-BuOOH at 50 °C; furthermore, reaction mechanisms were proposed for the Hantzsch reaction and the aromatization of 1,4-DHP.

## 2. Experimental

### 2.1. Catalyst preparation

Iron, cobalt and copper tetrasulfophthalocyanine complexes FePcS, CoPcS, and CuPcS were prepared following the method reported by Weber and Busch with slight modifications [35–37]. The sulphonated complexes were prepared by slowly addition (for around 1 h) of a fine grounded solid mixture of urea (23.2 g), ammonium chloride (1.9 g), ammonium heptamolibdate tetrahydrate (0.2 g), metal (II) sulfate heptahydrate (3.4 g) and monosodium salt of 4-sulfophthalic acid (17.3 g) to 24 mL of hot nitrobenzene (180 °C). The suspension was stirred at 180 °C for 7 h, then the dark solid paste was cooled to room temperature and washed with ethanol until no nitrobenzene smell was detected. Then, the solid was purified and dried under vacuum at room temperature. Iron hexadecachlorophthalocyanine, $FePcCl_{16}$, was synthesized following the method reported by Metz and coworkers [38]. A mixture of urea (11.7 g), tetrachlorophthalic anhydride (16 g), $FeCl_2{\cdot}4H_2O$ (2.8 g) and ammonium heptamolibdate tetrahydrate (0.1 g) was well grounded. The finely pulverized mixture was added to 50 mL of nitrobenzene, then the temperature of the mixture was increased to 180–190 °C within 30 min and this temperature was kept during 4 h until complete evolution of ammonia. The viscous olive green suspension was cooled to 90 °C, diluted with 50 mL of ethanol, and the solid was filtered hot. The solid recovered was copiously washed with boiling water until a clear filtrate was obtained. Finally, the solid was purified and dried overnight at 80 °C under vacuum. The complexes were immobilized on amorphous commercial fumed $SiO_2$ (Aldrich) and mesoporous silica SBA-15. The SBA-15 support was prepared using an amphiphilic $(EO)_{20}(PO)_{70}(EO)_{20}$ triblock copolymer (average molecular weight 5800, Aldrich) and tetraethylorthosilicate according to the method described in literature by Shah and coworkers [39]. The supports ($SiO_2$ and SBA-15) were modified with 3-aminopropyltriethoxysilane (APTES) following a reported procedures [40,41]: 3-APTES (2 mmol) was added to a suspension, in 40 mL of dry *m*-xylene, of 4.5 g of the siliceous materials previously treated at 200 °C under vacuum for 24 h. The final mixture was refluxed under argon for 15 h. The solids (named as $NH_2$-$SiO_2$ and $NH_2$-SBA-15) were separated by filtration, washed with acetone and dried at 80 °C under vacuum. Metallotetrasulfophthalocyanines (MPcS) were converted to metallotetrachlorosulfonylphthalocyanines ($MPc(SO_2Cl)_4$) before

**Table 1**
Metal content, UV–vis bands and $NH_3$ amount desorbed of several silica based materials.

| Material | Color | Metal content, μmol/g | $S_{total}$, $m^2/g$ | $NH_3$ desorbed, mmol/g |
|---|---|---|---|---|
| $SiO_2$ | White | 0 | 211 | 3.29 |
| SBA-15 | White | 0 | 755 | 10.9 |
| FePcS-$NH_2$-$SiO_2$ | Blue | 34.9 | 124[a] | 10.7 |
| CoPcS-$NH_2$-$SiO_2$ | Blue | 50.9 | 139[a] | 3.78 |
| CuPcS-$NH_2$-$SiO_2$ | Blue | 79.6 | 145[a] | 4.05 |
| $FePcCl_{16}$-$NH_2$-$SiO_2$ | Green | 62.6 | 137 | 13.2 |
| $FePcCl_{16}$-$NH_2$-SBA-15 | Green | 41.1 | 305 | 16.8 |

[a] Determined with a single point BET procedure and measured in a Micromeritics AutoChem II 2920.

immobilization as follows: MPcS (600 mg) was stirred with DMF (4 drops) and $SOCl_2$ (6 mL) under argon for 6 h at 50 °C. Then, the excess of chloride was removed by evaporation. The final solid was washed with toluene (20 mL) and dried under vacuum at room temperature for 24 h. MPc$(SO_2Cl)_4$ complexes were immobilized on $NH_2$-$SiO_2$ (FePcS-$NH_2$-$SiO_2$, CoPcS-$NH_2$-$SiO_2$, and CuPcS-$NH_2$-$SiO_2$) following reported procedures [42]. The obtained blue solids were filtrated, washed with water and acetone, and dried under vacuum at 80 °C for 24 h. For the synthesis of $FePcCl_{16}$-$NH_2$-$SiO_2$ and $FePcCl_{16}$-$NH_2$-SBA-15 catalysts, the $FePcCl_{16}$ complex was dissolved in pyridine (0.003 g complex/mL) and the system was stirred for 7 h at room temperature. Then, a suspension of the support (0.1 g/mL) in pyridine was stirred 5 min in a round bottom flask, and the complex-pyridine mixture was added to the suspension dropwise under argon flux. After complete addition of the complex, the new suspension was stirred at room temperature for 1 h, and then at reflux for 24 h. The green solid obtained after cooling was washed with acetone until a colorless filtrate was observed. Finally, the solid was dried under vacuum at 80 °C for 15 h.

### 2.2. Catalyst characterization

TGA (Thermal Gravimetric Analysis) was performed between 25 and 800 °C in a TGA Q500 V20. 13 BUILD 39 TA Instrument, under nitrogen flow. IR spectra were recorded in a Nicolet Avatar 330 FTIR with dispersive cell using a 3% diluted sample in KBr. Metal content of catalysts was determined by atomic absorption in a Model S4 spectrometer from Thermoelectron Corporation. Diffuse reflectance UV–vis spectra were carried out using a Perkin-Elmer Lambda 9 spectrometer (200–800 nm) without further sample treatment. $N_2$ adsorption/desorption data were collected in an ASAP 2010 equipment. $NH_3$-TPD (Temperature-Programmed Desorption of $NH_3$) analyses were carried out in an Autochem II 2920; the sample (0.05 g) was loaded in a quartz tube, and then pretreated in 50 mL/min flowing argon (99.99%) up to 300 °C for 1 h at 10 °C/min. Samples were then cooled to 50 °C and saturated with 50 mL/min $NH_3$ (0.3% in He) for 1 h. $NH_3$ loosely bound to the surface was removed by flowing 50 mL/min of He for 1 h at 10 °C/min up to 1050 °C. Small angle XRD for SBA-15 materials was collected in a Bruker Smart Apex CCD-based diffractometer system. For the SEM (Scanning Electron Microscopy) image a JEOL model JFM-6490LV equipment was used. Raman spectra were collected in a Horiba Jobin Yvon Labram HR spectrometer using a 633 nm He–Ne laser.

### 2.3. Catalytic reactions

The Hantzsch reaction was carried out in solvent-free conditions. The aldehyde (1 mmol), **1**, methyl or ethyl acetoacetate (2 mmol), **2**, and a light excess of ammonium acetate (1.3 mmol), **3**, were mixed with the catalyst (0.05–0.2% mmol) in a round bottom flask, and they were stirred at 200 rpm for 24 h at constant temperature (25–105 °C). The samples were collected from the flask during the reaction at time intervals. For the oxidation of the 1,4-DHPs, the catalyst (1% mmol) was mixed with the 1,4-DHPs and *t*-BuOOH (molar ratio 1:5) in acetonitrile at 50 °C. The reactions were monitored by gas chromatography (GC) with a Shimadzu GC-2014 equipment using a SPB-1 capillary column (30 m × 0.32 mm). Conversion was defined as the ratio of converted species (**6**, **7**, **8** and/or **9**, according to Fig. 1) with respect to the initial concentration of the aldehyde. The products were identified by comparison of their melting points, chromatographic and spectroscopic data (TLC, NMR) with those reported values [43]. For $^{13}C$ NMR and $^{1}H$ NMR spectra, tetramethylsilane (TMS) was used as internal stan-

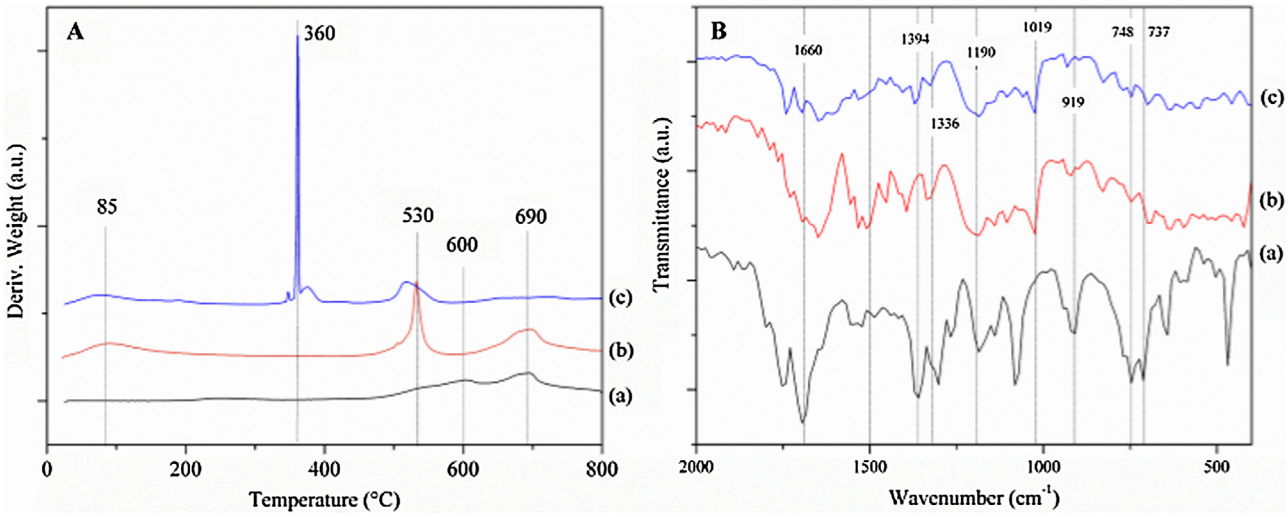


**Fig. 3.** TGA profiles (A) and FT-IR spectra (B) of complexes: $FePcCl_{16}$ (a), FePcS (b), and CoPcS (c).

dard (Supplementary information, S1). In the reusing reactions, the catalyst was filtered after each reaction, washed with acetonitrile and dried in a vacuum oven at 20 °C, before a subsequent use.

## 3. Results and discussion

### 3.1. Catalyst characterization

Thermogravimetric analysis (TGA) and FT-IR spectroscopic analysis were used for determining the success in the synthesis of the phthalocyanine complexes, FePcS, CoPcS, and $FePcCl_{16}$, Fig. 3. The phthalocyanines have a decomposition temperature higher than 500 °C [44,45] because of the high thermal stability of this molecule owing to the extended π system of the phthalocyanine structure [44]. The presence of chlorine in the periphery of $FePcCl_{16}$ increases the stability of the complex [46] and gives a higher decomposition temperatures respect to the sulfonated complexes, Fig. 3A (curve a); $FePcCl_{16}$ complex presented two decomposition peaks at 600 °C and 690 °C. In the case of the tetrasulfonated complexes, the peak between 70 °C and 100 °C, Fig. 3A (curves b and c), is due to desorption of water [47]. Decomposition of the complexes was observed at 560 and 730 °C (FePcS) and 360 and 525 °C (CoPcS) [48,49]. Fig. 3B shows the infrared spectra of FePcS, CoPcS, and $FePcCl_{16}$ complexes. The band at 1660 $cm^{-1}$ is assigned to the C—C stretching vibration in pyrrole and the bands at 1394 $cm^{-1}$ and 1336 $cm^{-1}$ are attributed to C—C stretching in isoindole [24,50]. The band around 1500 $cm^{-1}$ is assigned to the C—H bending in aryl [50]. The bands at 1190 $cm^{-1}$ and 1019 $cm^{-1}$ belong to C—N stretching vibration and in pyrrole, respectively [50]. Metal-nitrogen stretching was confirmed with the band at around 919 $cm^{-1}$ [51]. In the of $FePcCl_{16}$ complex its FTIR complex, Fig. 3B (curve a), showed additional bands at 923 $cm^{-1}$ associated to M—N vibrations [51], and bands at 748 and 737 $cm^{-1}$ relate to C—Cl vibrations [52].

The immobilization of the complexes on the functionalized silicas was evidenced by the color changes, as well as by the chemical analysis of metal, BET surface area, UV–vis and Raman Spectroscopies. The color of the immobilized phthalocyanines ranged between blue and green, Table 1; these colors are attributed to the ligand transitions π–π* of the C—N bonds in the phthalocyanine ring [36]. Blue color and UV–vis bands (Fig. 4) between 630 and 642 nm confirm the presence of μ-oxo dimeric species in the catalyst [42]; meanwhile, green color and UV–vis bands between 400–500 nm or between 660–680 nm are associated with monomeric species immobilized on the supports [36]. In addition, all immobilized complexes showed a band at around 350 nm (assigned to the π–π transition of C=C double bond [51]), suggesting that the complex remained intact during the immobilization process.

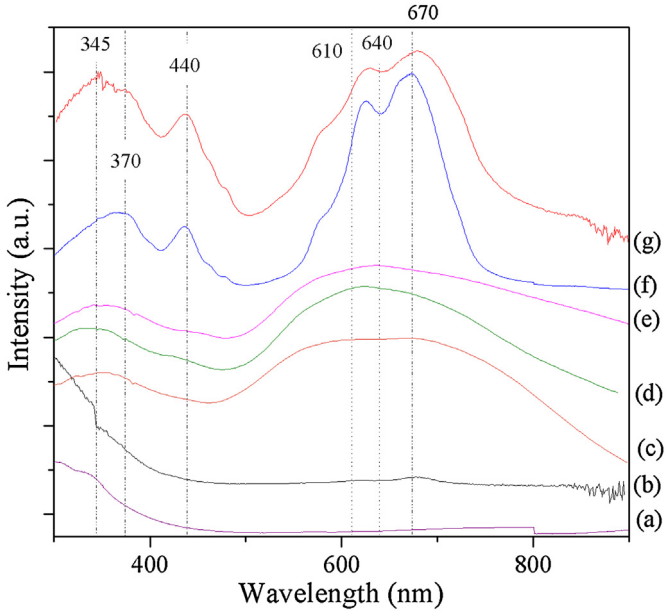


**Fig. 4.** UV–Vis spectra for supported catalysts: $NH_2$-$SiO_2$ (a), $NH_2$-SBA-15 (b), CoPcS-$NH_2$-$SiO_2$ (c), CuPcS-$NH_2$-$SiO_2$ (d), FePcS-$NH_2$-$SiO_2$ (e), $FePcCl_{16}$-$NH_2$-$SiO_2$ (f), and $FePcCl_{16}$-$NH_2$-SBA-15 (g).

Fig. 4 The incorporation of the metal complex into the silica causes a decrease in surface area (Table 1) most notably in the case of the $FePcCl_{16}$-$NH_2$-SBA-15 due to the partial blocking of the mesopores by the incorporated complex. The pore size distribution of

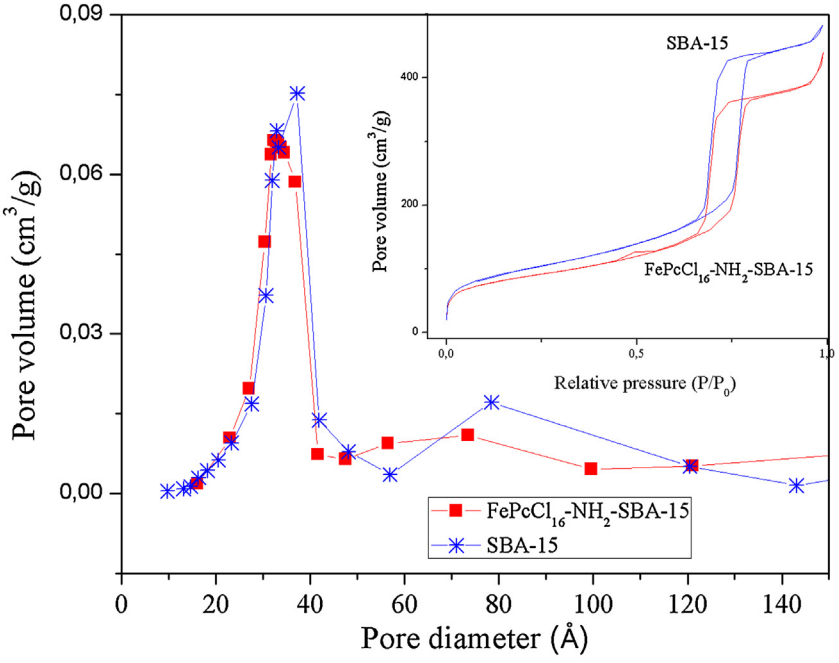


**Fig. 5.** Pore size distribution (A) and nitrogen adsorption isotherm (B) of SBA-15 and $FePcCl_{16}$-$NH_2$-SBA-15.

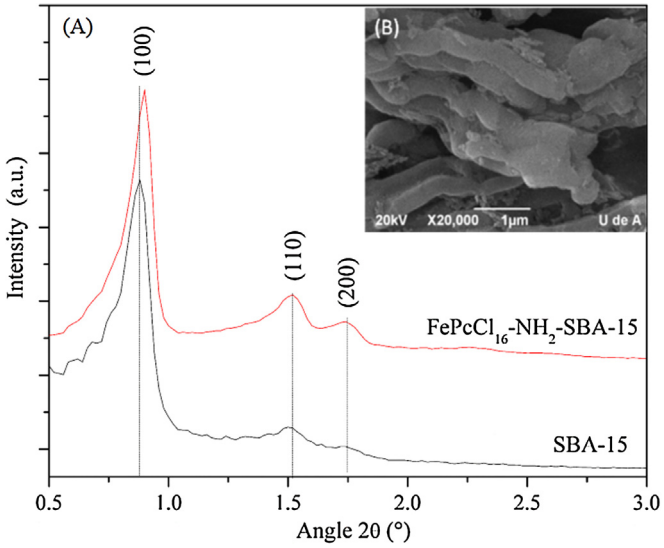


**Fig. 6.** Small angle XRD (A) of synthesized SBA-15 and $FePcCl_{16}$-$NH_2$-SBA-15, and SEM image (B) of $FePcCl_{16}$-$NH_2$-SBA-15.

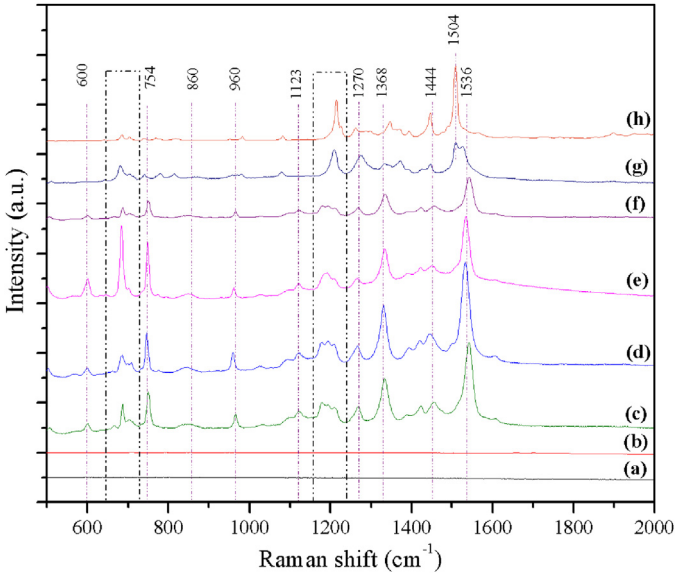


**Fig. 7.** Raman analysis of supported catalysts: $NH_2$-$SiO_2$ (a), $NH_2$-SBA-15 (b), CoPcS-$NH_2$-$SiO_2$ (c), CuPcS-$NH_2$-$SiO_2$ (d), FePcS-$NH_2$-$SiO_2$ (e), FePcS-$NH_2$-$SiO_2$ used in Hantzsch reaction (f), $FePcCl_{16}$-$NH_2$-$SiO_2$ (g), and $FePcCl_{16}$-$NH_2$-SBA-15 (h).

$FePcCl_{16}$-$NH_2$-SBA-15 and SBA-15 are similar; the decrease in the pore volume confirms the incorporation of the complex into the channels, Fig. 5A, [51]. $FePcCl_{16}$-$NH_2$-SBA-15 presents the typical irreversible-type IV adsorption isotherm with H1 hysteresis loop [40,51], related with typical mesoporous structures of uniform pore size, Fig. 5B, but with a less porous volume in comparison with SBA-15. In addition, XRD pattern of SBA-15 materials indicates a good mesoscopic order of the materials and that the characteristic hexagonal features of SBA-15 are maintained in $FePcCl_{16}$-$NH_2$-SBA-15, Fig. 6A [40]. Besides, SEM image of the $FePcCl_{16}$-$NH_2$-SBA-15 (Fig. 6B) shows the typical rope-like domains aggregated into a wheat-like microstructure of SBA-15 [40].

Raman analysis confirms the incorporation of the complexes in the supports, Fig. 7, since not absorption bands are observed in $NH_2$-$SiO_2$ (curve a) and $NH_2$-SBA-15 (curve b). In this analysis, a laser at 633 nm closer to the resonance with the main Q absorption band of phthalocyanine was used. The band at 600 $cm^{-1}$ is associated to the ring breathing, N—M stretching and benzene expending [53]. The Pc ring "breathing" at around 650–730 $cm^{-1}$ is observed in all materials but mainly in the sulphonated materials [54–56]. The strong band at 754 $cm^{-1}$ is assigned to $C_\alpha$–$N_\alpha$–$C_\alpha$ bonds [58]. The weak band at around 860 $cm^{-1}$ is referred with both the coupling of isoindole deformation and with the aza stretching C—H bend [54–56]. The weak band at 960 $cm^{-1}$ is associated to isoindole deformation [58]. The weak band at 1123 $cm^{-1}$ is due to C—H in-plane bending [58]. The strong bands at around 1158–1240 $cm^{-1}$ are typically associated to C—H bend, vibrational frequencies derived from isoindole ring stretching and the aza group stretching [53,58]. Medium bands in the range of 1299–1322 $cm^{-1}$ correspond to C=C pyrrole and benzene stretching, and weak and medium bands at around 1368–1444 $cm^{-1}$ is referred to isoindole stretching [54]. The Raman band found at 1536 $cm^{-1}$ is correlated to the displacement of the C—$N_\alpha$–C bonds of the phthalocyanine ring [57]. In the case of $FePcCl_{16}$ catalysts the strong bands at around 1504 $cm^{-1}$ correspond to coupling of pyrrole and aza stretching [54–56], and the bands between 650 and 730 $cm^{-1}$ can be also associated with the C—Cl stretch in the Pc periphery [59].

The acidity of the catalyst has an important influence on the efficiency of the Hantzsch reaction [11,60]. The acid properties of the catalyst were examined by $NH_3$-TPD, the desorbed $NH_3$ (Table 1) corresponds to the amount of acid sites whereas

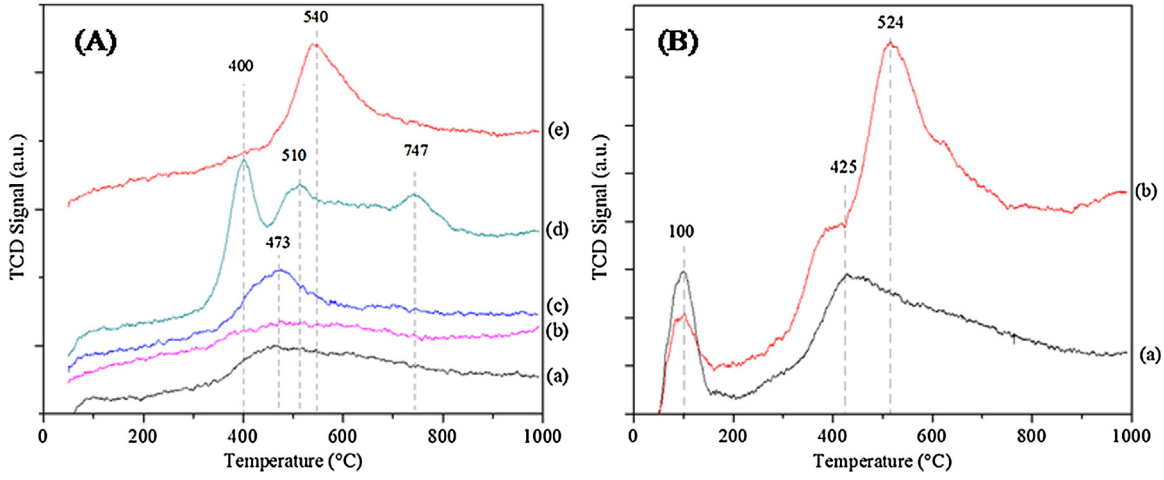


**Fig. 8.** $NH_3$-TPD profiles of silica and SBA-15 supported catalysts. In (A), $SiO_2$ (a), FePcS-$NH_2$-$SiO_2$ (b), CoPcS-$NH_2$-$SiO_2$ (c), CuPcS-$NH_2$-$SiO_2$ (d), and $FePcCl_{16}$-$NH_2$-$SiO_2$ (e). In (B), SBA-15 (a) and $FePcCl_{16}$-$NH_2$-SBA-15 (b).

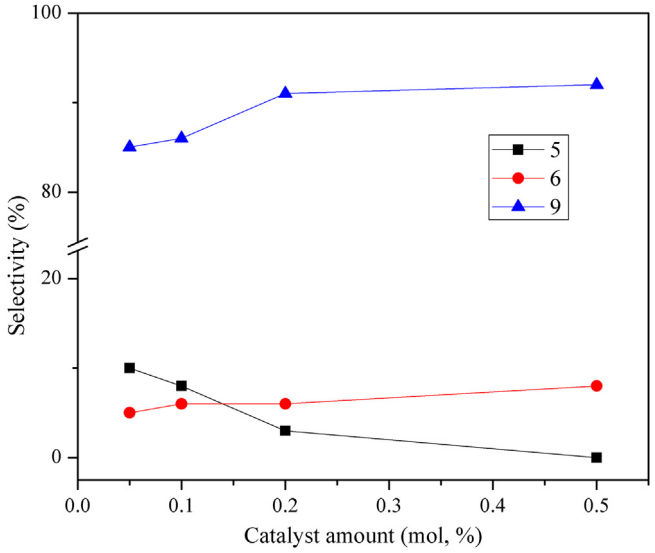


**Fig. 9.** Effect of the FePcS-$NH_2$-$SiO_2$ catalyst concentration on the selectivity in the Hantzsch reaction. Reaction conditions: Benzaldehyde (1 mmol), methyl acetoacetate (2 mmol), ammonium acetate (1.2 mmol), catalyst, solvent-free, 25 °C, magnetic stirring (200 rpm), 24 h. Benzaldehyde conversion was 100%. Selectivities to 7 and 8 were 0%. Compound 4 was not detected under GC analysis conditions.

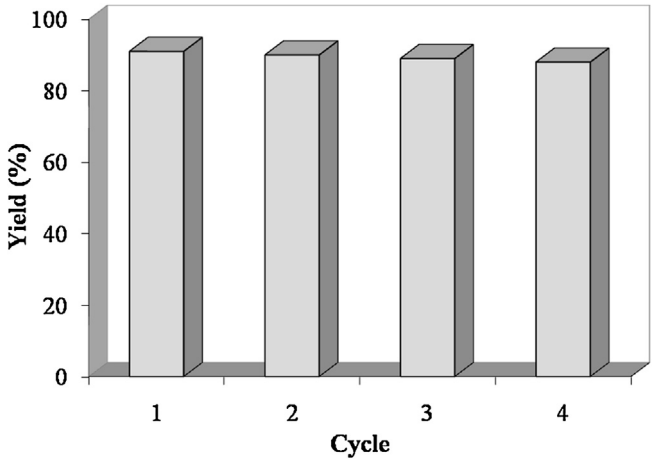


**Fig. 10.** Yield to 2-phenylpyridine **9** in reusing tests of FePcS-$NH_2$-$SiO_2$ catalyst. Reaction conditions: Benzaldehyde (1 mmol), methyl acetoacetate (2 mmol), ammonium acetate (1.2 mmol), catalyst (0.2%), solvent-free, 25 °C, magnetic stirring (200 rpm), 24 h. Benzaldehyde conversion was 100%. Catalyst lost lower than 5% after each reuse.

the peak position in the profile, Fig. 8, indicates the strength of the acid sites: weak (180–250 °C), medium (280–330 °C) or strong (380–500 °C) [61]. However, by $NH_3$-TPD analysis it is not possible to distinguish between Brönsted and Lewis acidity [61]. According with the results presented in Table 1, the acidity of the support increased after incorporation of the complex. In the case of $SiO_2$-supported catalysts, the acidity decreased in the following order: FePcCl$_{16}$-$NH_2$-$SiO_2$ > FePcS-$NH_2$-$SiO_2$ > CuPcS-$NH_2$-$SiO_2$ > CoPcS-$NH_2$-$SiO_2$. This behavior can be associated with the electron withdrawing effect of Cl atoms, which is higher than the effect in sulphonated complexes [62]. According with Fig. 8, all the materials supported on silica showed strong acidity. Moreover, the peaks over 500 °C suggested the strong interaction between the $NH_3$ and the metallic center in the phthalocyanine [63]. In the particular case of the CuPcS-$NH_2$-$SiO_2$ catalyst, the presence of different desorption peaks, Fig. 8A, means that there exist several competing adsorption sites for ammonia [63]. $NH_3$-TPD of catalyst supported on SBA-15, Fig. 8B, has a similar behavior than silica-supported catalysts. An additional peak at 100 °C is observed in both bare and supported SBA-15. This typical peak in SBA-15 [64] is associated to desorption of hydrogen-bonded $NH_3$ [65].

**Table 2**
Effect of the metal on the activity of MPcS-$NH_2$-$SiO_2$ catalysts in the Hantzsch reaction.

| Catalyst | Time (h) | Selectivity (%) | | | |
|---|---|---|---|---|---|
| | | **5** | **6** | **7** | **9** |
| None | 60[a] | 15 | 0 | 0 | 74 |
| FePcS-$NH_2$-$SiO_2$ | 4 | 36 | 5 | 5 | 52 |
| | 8 | 13 | 6 | 20 | 61 |
| | 12 | 8 | 6 | 10 | 76 |
| | 24 | 3 | 6 | 0 | **91** |
| CoPcS-$NH_2$-$SiO_2$ | 4 | 58 | 7 | 9 | 26 |
| | 8 | 30 | 7 | 22 | 40 |
| | 12 | 5 | 8 | 11 | 76 |
| | 24 | 0 | 9 | 0 | **91** |
| CuPcS-$NH_2$-$SiO_2$ | 4 | 47 | 7 | 24 | 22 |
| | 8 | 29 | 7 | 27 | 37 |
| | 12 | 10 | 7 | 15 | 68 |
| | 24 | 7 | 0 | 0 | **85** |

Reaction conditions: Benzaldehyde (1 mmol), methyl acetoacetate (2 mmol), ammonium acetate (1.2 mmol), catalyst (0.2%), solvent-free, 25 °C, magnetic stirring (200 rpm). Compound **4** was not detected under GC analysis conditions. Benzaldehyde conversion was 100% after 4 h in the presence of catalysts. [a]Time for obtaining 100% conversion of benzaldehyde and selectivity to **8** was 11%. The bold numbers represent the maximum selectivity obtained for compound **9** over each tested catalyst.

### 3.2. Catalytic Hantzsch reactions

The presence of the catalyst in the reaction medium has an important effect on the benzaldehyde conversion since complete conversion (100%) is obtained after 4 h at room temperature (Table 2). When the supported metallosulphonated phthalocyanines (MPcS-$NH_2$-$SiO_2$) are used as catalysts, the reaction is under kinetic control and the main product obtained corresponds to 2-phenylpyridine, **9,** formed through a 1,2-addition and subsequent oxidation reaction [11]. Formation of **9** takes place through a tandem reaction (Fig. 1) in which the heterocycle **7** is first formed and then it is aromatized due to the air present in the reactor [11].

The results in Table 2 show that in each step of the tandem reaction the corresponding 'individual reaction rate' depends on the metal present in the used catalyst, as it confers different final properties to the material. The formation of the intermediate compound **5** is faster over CoPcS-$NH_2$-$SiO_2$, the catalyst with the lowest acidity (Table 1). In the case of the 1,2-addition reaction step (involved in the formation of the 1,2-DHP) the copper catalyst showed the highest product formation. This fact could be associated with the strong acidic sites present in the CuPcS-$NH_2$-$SiO_2$ catalyst since they are important in the synthesis of 1,2-DHPs compounds [66]. Regarding to the final step, the oxidation of the 1,2-DHP to the 2-phenylpyridine, **9**, is faster over FePcS-$NH_2$-$SiO_2$, followed by CoPcS-$NH_2$-$SiO_2$ and CuPcS-$NH_2$-$SiO_2$ catalysts. These results show that under aerobic conditions the MPcS-$NH_2$-$SiO_2$ catalysts can effectively oxidize the 1,2-DHP with oxygen as stoichiometric oxidant [67,68], and the intensity of its activity can be related with both the electronegativity of the metal center and the capability to form an adduct with the oxygen atom for the abstraction of the hydrogen as in allylic oxidation [62].

Comparing the activity of FePcS-$NH_2$-$SiO_2$ and FePcCl$_{16}$-$NH_2$-$SiO_2$ in each step of the tandem reaction (Table 2 and Table 3, respectively), the strongest acid strength of the chlorinated complex can be directly related with the highest addition reaction rate observed. The electron-withdrawing effect of the chlorine atoms

**Table 3**
Effect of the support on the activity of $FePcCl_{16}$ complex in the Hantzsch reaction.

| Catalyst | Time (h) | Selectivity (%) | | | |
|---|---|---|---|---|---|
| | | **5** | **6** | **7** | **9** |
| $FePcCl_{16}$-$NH_2$-$SiO_2$ | 4 | 22 | 14 | 39 | 21 |
| | 8 | 8 | 15 | 50 | 26 |
| | 12 | 3 | 15 | 17 | 65 |
| | 24 | 0 | 17 | 0 | **83** |
| $FePcCl_{16}$-$NH_2$-SBA-15 | 4 | 35 | 5 | 44 | 15 |
| | 8 | 21 | 5 | 35 | 40 |
| | 12 | 12 | 5 | 17 | 66 |
| | 24 | 0 | 6 | 0 | **94** |

Reaction conditions: Benzaldehyde (1 mmol), methyl acetoacetate (2 mmol), ammonium acetate (1.2 mmol), catalyst (0.2%), solvent-free, 25 °C, magnetic stirring (200 rpm). Benzaldehyde conversion was 100% after 4 h. Selectivity to **8** was 0%.). Compound **4** was not detected under GC analysis conditions. The bold numbers represent the maximum selectivity obtained for compound **9** over each tested catalyst.

in Fe gives a decrease in the oxidation rate through the formation of the 2-phenylpyridine, since its formation is lower over the $FePcCl_{16}$-$NH_2$-$SiO_2$ catalyst, Table 3 [33]. In addition, with this chlorinated catalyst the selectivity to 1,4-DHP compound **6** suggests the presence of active sites which favor mainly the Michael addition. An important effect of both acidity and support seems to be the responsible of the high activity of the $FePcCl_{16}$-$NH_2$-SBA-15 catalyst (Table 3).

**Table 4**
Effect of the temperature on the selectivity in the Hantzsch reaction over FePcS-$NH_2$-$SiO_2$ catalyst.

| Entry | Temperature (°C) | Selectivity (%) | | | | |
|---|---|---|---|---|---|---|
| | | **5** | **6** | **7** | **8** | **9** |
| 1 | 0 | 43 | 5 | 4 | 0 | 48 |
| 2 | 25 | 36 | 5 | 5 | 0 | 52 |
| 3 | 45 | 0 | 30 | 0 | 0 | 70 |
| 4 | 65 | 0 | 47 | 0 | 0 | 53 |
| 5 | 85 | 0 | 53 | 0 | 0 | 47 |
| 6 | 105 | 0 | 55 | 0 | 15 | 35 |

Reaction conditions: Benzaldehyde (1 mmol), methyl acetoacetate (2 mmol), ammonium acetate (1.2 mmol), catalyst (0.2%), solvent-free, magnetic stirring (200 rpm), 24 h. Benzaldehyde conversion was 100%). Compound **4** was not detected under GC analysis conditions.

Temperature has an important effect on the selectivity in the Hantzsch reaction [11,12]. Over FePcS-$NH_2$-$SiO_2$ and after 24 h of reaction (Table 4), an increase in reaction temperature causes the rise of 1,4-DHPs formation. At low temperatures (entries 1 and 2)

**Table 5**
Activity of FePcS-$SiO_2$ catalyst in the synthesis of 2-phenylpyridines.

| Entry | Aldehyde | Product[a] | Yield (%)[b] | Melting point (°C) or color | |
|---|---|---|---|---|---|
| | | | | This work | Reported, [15] |
| 1[c] | 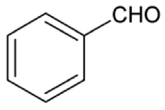 | 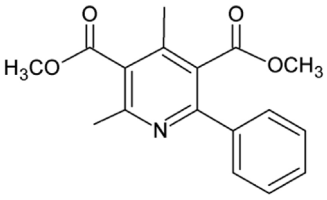 | 90 | 85-87 | 85.0-86.2 |
| 2[c] | 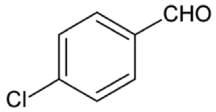 | 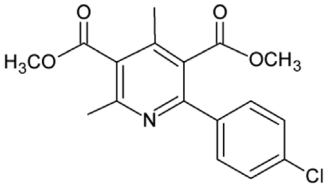 | 84 | 87-90 | 81.9-90.2 |
| 3[c] | 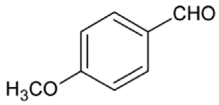 | 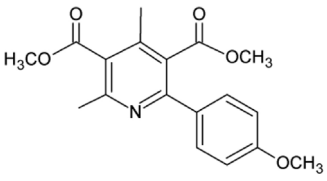 | 71 | Colorless oil | Colorless oil |
| 4[d] | 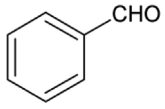 | 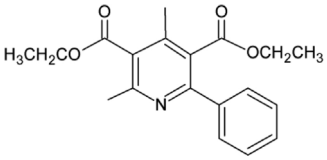 | 92 | Colorless oil | Colorless oil |
| 5[d] | 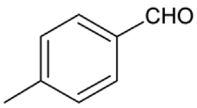 | 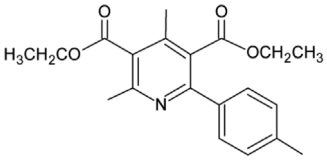 | 83 | 49-50 | 49.1-50.3 |

[a] Characterization in Supplementary information, S1.
[b] Corresponding aldehyde conversion was 100%. Reaction conditions: Aldehyde (1 mmol).
[c] Methyl acetoacetate (2 mmol).
[d] Ethyl acetoacetate (2 mmol), ammonium acetate (1.2 mmol), FePcS-$SiO_2$ (0.2 mol %), solvent-free, air atmosphere, 25 °C, magnetic stirring (200 rpm), 24 h.

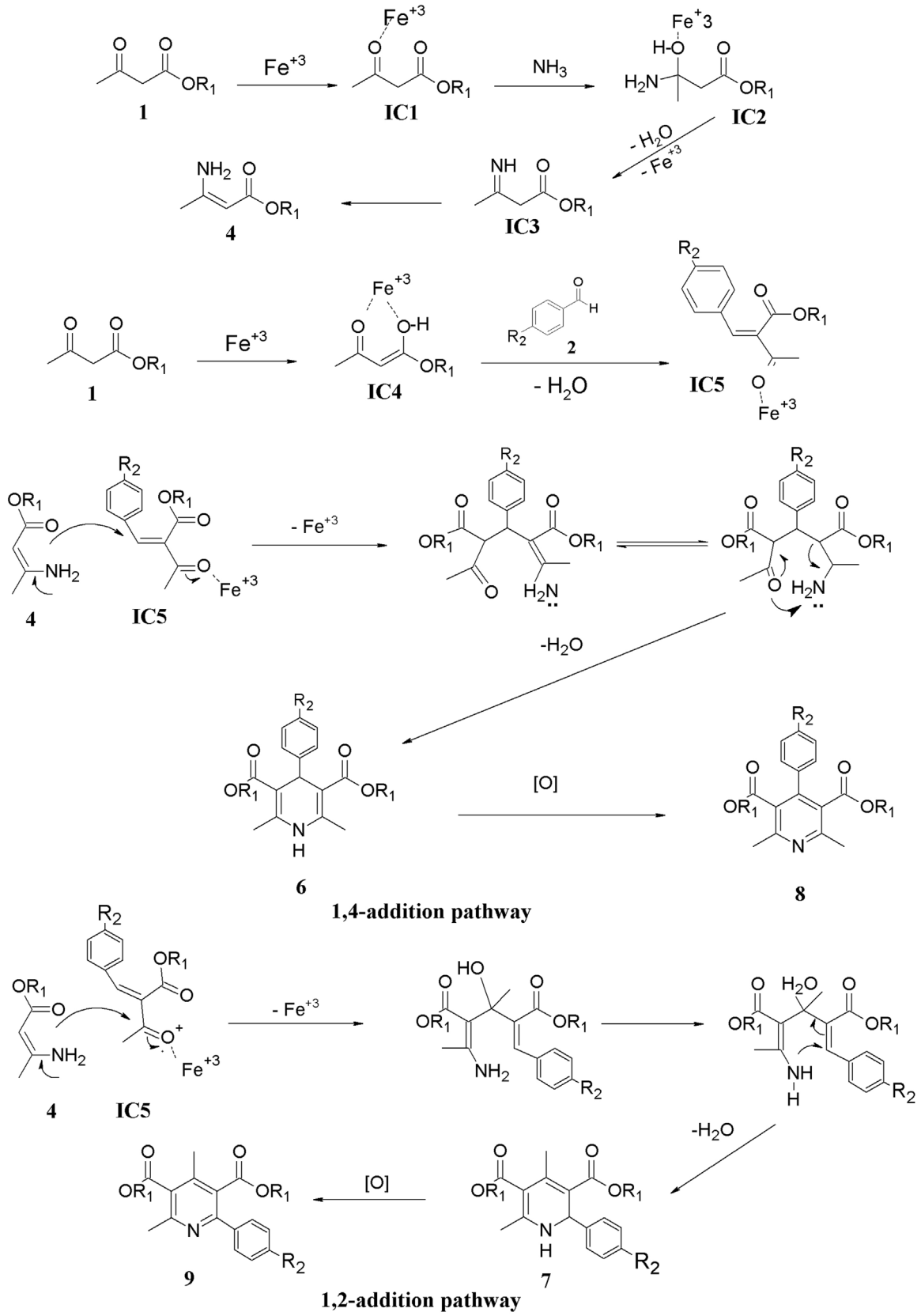


**Fig. 11.** Proposed mechanism for Hantzsch reaction over FePcS-$NH_2$-$SiO_2$ catalyst.

the 1,2-addition is more important (kinetic control) but at higher temperatures (entries 5 and 6), the 1,4-addition is greater (thermodynamic control). At 45 and 65 °C, the presence of the 1,4-DHP, **6**, becomes important (entries 3 and 4). Only at 105 °C, the oxidation of 1,4-DHP is observed (entry 6).

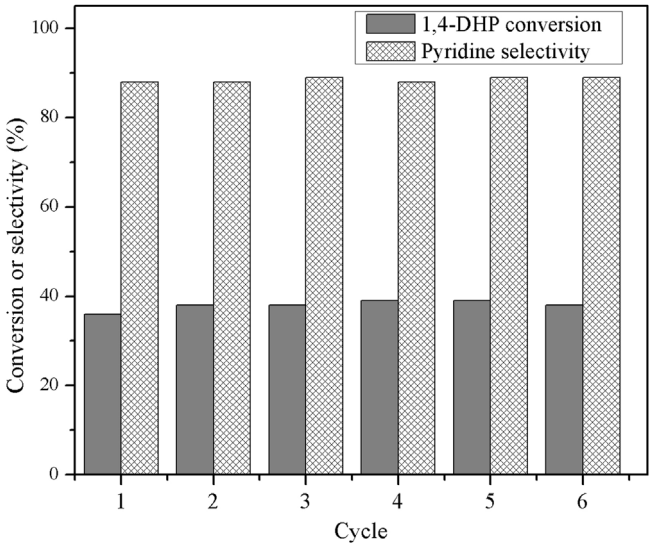


**Fig. 12.** Stability of FePcS-$NH_2$-$SiO_2$ catalyst in the aromatization of 2,6-dimethyl-3,5- dicarbomethoxy-4-phenyl-1,4-dihydropiridine with *t*-BuOOH. Reaction conditions: 1,4-DHP (1 mmol), t-BuOOH in decane (5.5 M) (5 mmol), acetonitrile as solvent, 50 °C, 6 h. Before reusing, the catalyst was washed with acetonitrile and dried in a vacuum oven at 20 °C.

The amount of active sites that are available in the reaction medium is an important issue. When the concentration of FePcS-$NH_2$-$SiO_2$ increases in the Hantzsch reaction (Fig. 9), the selectivity to the Knoevenagel condensation product **5** decreases and the selectivity to 2-phenylpyridine increases. This fact could suggest that the catalyst role in the 1,2-addition is important; however, the effect is only appreciable until a 0.2 mol % catalyst concentration. With a catalyst concentration of 0.2 mol % the 2-phenylpyridine selectivity was 91% and it only increased in a 1% with 0.5 mol % of catalyst. Finally, a good stability of the FePcS-$NH_2$-$SiO_2$ catalyst was found; not appreciable lost in 2-phenylpyridine, **9**, yield was detected after at least 4 reuses, Fig. 10; furthermore, Raman analysis of the catalyst after reuses (Fig. 7, curve f) was very similar to the fresh catalyst.

In this study, a yield of 2-phenylpyridine, **9,** higher than 90% over the FePcS-$NH_2$-$SiO_2$ catalyst at room temperature (25 °C) in absence of solvent and after 24 h of reaction was obtained. Since the search of new methods for the synthesis of 2-phenylpyridines is highly desirable [10,11], the Hantzsch reaction over FePcS-$NH_2$-$SiO_2$ was tested with different aldehyde precursors (Table 5). According with the obtained results, an important improvement of the reaction was achieved respect to previously reported catalytic systems: similar or even better yields to 2-phenylpyridines were achieved at lower reaction times (24 h) in comparison with the results reported by Cao and coworkers after 72 h of reaction [10].

A plausible mechanism based on the Lewis acid sites ($Fe^{3+}$) of the FePcS-$NH_2$-$SiO_2$ catalyst is presented in Fig. 11, since these iron sites facilitate the Hantzsch reaction [12]. The β-dicarbonyl compound, **1**, promotes the formation of different intermediate compounds (**IC1–IC5**) with the catalyst. The formation of the ester enamine (**4**) is due to the condensation of a β-dicarbonyl-catalyst adduct with ammonia (derived from a **3**). The Knoevenagel condensation between β-dicarbonyl-catalyst (**IC4**) and the aldehyde **2** led to the formation of the intermediate compound with the catalyst (β-dicarbonyl-catalyst-aldehyde) **IC5**. Further condensations between the ester enamine (**4**) and the intermediate compound **IC5** give the formation of the 1,4 addition product 1,4-dihydropyridine, **6**, or the 1,2-addition to form the 1,2-dihydropyridine, **7** [11]. According with the experimental results, the addition of the ester enamine (**4**) in the intermediate compound **IC5** is favored in the 1,2-position. Finally, the aromatization for obtaining the corresponding pyridines **8** and **9**, can be associated with the air from the media which can also form the oxidized $Fe^{IV}$ = O specie [62,67].

**Table 6**
Activity of FePcS-$NH_2$-$SiO_2$ catalyst in the direct oxidation of 1,4-DHPs to pyridines with *t*-BuOOH.

| Entry | Conversion of 1,4-DHP (%) | Pyridine[a] | Selectivity to pyridine (%) |
|---|---|---|---|
| 1[b] | 35 | 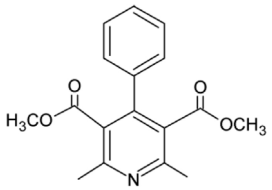 | 88 |
| 2 | 38 | 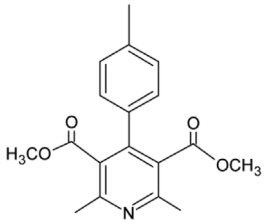 | 91 |
| 3 | 36 | 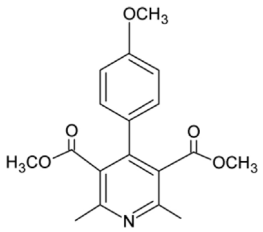 | 93 |
| 4 | 37 | 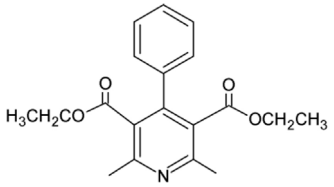 | 92 |
| 5 | 36 | 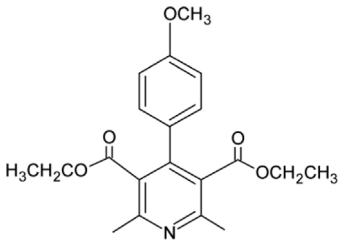 | 93 |

[a] Characterization in Supplementary information, S1.
[b] Previously reported [40]. Reaction conditions: 1,4-DHP (1 mmol), *t*-BuOOH in decane (5.5 M) (5 mmol), acetonitrile as solvent, 50 °C, 6 h.

### 3.3. Catalytic aromatization of 1,4-DHPs

As it was observed above (Table 4), oxidative dehydrogenation of 1,4-DHP **6** to pyridine **8** was achieved at 105 °C with only 15% of product selectivity; this suggests that the catalytic system FePc/air is not suitable for the aromatization of the 1,4- DHP. Therefore, in this section we evaluated the efficiency of *t*-BuOOH as oxidizing agent when FePcS-$NH_2$-$SiO_2$ is used as catalyst (Table 6).

As it was previously reported [69], the catalytic system FePcS-$NH_2$-$SiO_2$/*t*-BuOOH showed a good activity in the oxidation of 2,6-dimethyl-3,5-dicarbomethoxy-4-phenyl-1,4-dihydropiridine to its

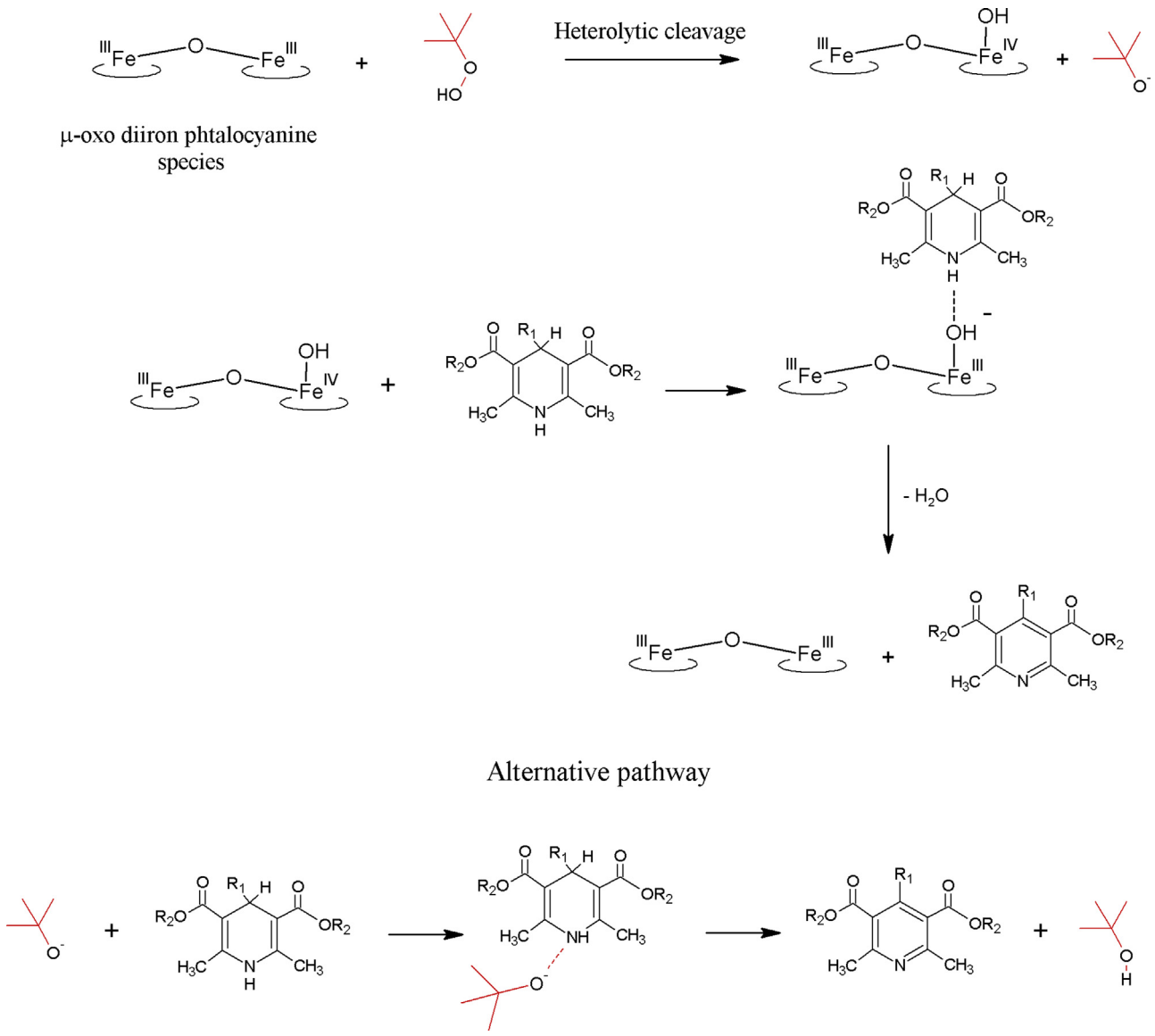


**Fig. 13.** Proposed mechanism for the 1,4-DHPs aromatization with FePcS-$NH_2$-$SiO_2$/t-BuOOH catalytic system.

pyridine maintaining a conversion near to 35% and selectivity value to its pyridine of 88% (Table 6, entry 1). According with Table 6, similar conversion (around of 36%) of the 1,4-DHPs is obtained with this catalytic system; however the selectivity to the corresponding pyridine depends on the type of R substituent and their electron donating effect on the 1,4-DHP [70]. The selectivity order is in agreement with electron donating effect in the aldehyde, $-OCH_3 > -CH_3 > -H$. Although the conversions are low (near to 35%), high pyridine selectivities are obtained, which corresponds to a desirable condition in organic transformations. When conversion increased, unknown secondary products began to appear (data not shown).

Good stability of the catalyst FePcS-$NH_2$-$SiO_2$ in the aromatization reaction of 1,4-DHPs was also observed (Fig. 12), since no appreciable lost in the oxidation of the 2,6-dimethyl-3,5-dicarbomethoxy-4-phenyl-1,4-dihydropiridine was detected after 6 reuses.

Analyzing our results and comparing with literature data for similar 1,4-DHPs aromatization reactions [71] and the oxidation species obtaining after the heterolytic cleavage of *t*-BuOOH due to the μ-oxo species of FePcS-$NH_2$-$SiO_2$ [14], a mechanism for the interaction between 1,4-DHP derivatives bearing an H substituent at the $N_1$-position and Fe=O can be postulated (Fig. 13). In addition, the free radical species formed *t*-$BuO^-$ could also abstracted the hydrogen from the 1,4-DHP and promoted the aromatization.

## 4. Conclusions

Metallo-sulphonated phthalocyanines (FePcS-$NH_2$-$SiO_2$, CoPcS-$NH_2$-$SiO_2$, and CuPcS-$NH_2$-$SiO_2$) and iron hexadecachlorinated phthalocyanines (FePc$Cl_{16}$-$NH_2$-$SiO_2$ and FePc$Cl_{16}$-$NH_2$-SBA-15) supported on siliceous materials were successfully synthesized and suitable used as catalysts for the multicomponent Hantzsch reaction between benzaldehyde, methyl acetoacetate, and ammonium acetate, with a high selectivity to 2-phenylpyridine, **9**, at room temperature without solvent after 4 h of reaction. In the case of the FePcS-$NH_2$-$SiO_2$ catalyst, the 1,4-addition can be favored at temperatures higher than 65 °C. In the synthesis of the 2-phenylpyridine, the catalyst FePcS-$NH_2$-$SiO_2$ was reused in four consecutive runs with no appreciable loss of activity. The protocol for the synthesis of 2-phenylpyridines with different aldehydes over the catalyst FePcS-$NH_2$-$SiO_2$ was successfully applied with

yields over 70% after 24 h of reaction. In the 1,4-DHPs aromatization with the catalytic system FePcS-$NH_2$-$SiO_2$/*t*-BuOOH, the conversion (around of 35%) was independent on the employed precursor but the electron donating nature of the R substituent in the aldehyde affected the selectivity. In addition, the catalyst FePcS-$NH_2$-$SiO_2$ can be reused also at least six times in aromatization reaction without an appreciable loss of activity.

## Acknowledgments

The authors are grateful for the financial support to CONICET, UNLP and ANPCyT of Argentina (LMS, AGS, and GPR), and Universidad de Antioquia, UdeA, in Colombia (LMG and ALV).

## Appendix A. Supplementary data

Supplementary data associated with this article can be found, in the online version, at http://dx.doi.org/10.1016/j.mcat.2017.03.010.

## References

[1] F.C. Yu, B. Zhou, H. Xu, K.J. Chang, Y. Shen, Tetrahedron Lett. 56 (2015) 837–841.
[2] G.F. Zou, Z.P. Hu, S.Q. Zhang, W.W. Liao, Tetrahedron Lett. 56 (2015) 937–940.
[3] J.G. Breitenbucher, G. Figliozz, Tetrahedron Lett. 41 (2000) 4311–4315.
[4] S. Bahekar, S. Devanand, Acta Pharm. A (Zagreb, Croatia) 4 (2002) 281–287.
[5] M. Khoshneviszadeh, N. Edraki, K. Javidnia, A. Alborzi, B. Pourabbas, J. Mardaneh, R. Miri, Bioorg. Med. Chem. 17 (2009) 1579–1586.
[6] S. Gullapalli, P. Ramarao, Neuropharmacology 42 (2002) 467–475.
[7] G.H. Henry, Tetrahedron 60 (2004) 6043–6061.
[8] V.N. Kozhevnikov, D.N. Kozhevnikov, T.V. Nikitina, V.L. Rusinov, O.N. Chupakhin, M. Zabel, B.A. König, J. Org. Chem. 68 (2003) 2882–2888.
[9] V. Ahluwalia, B. Goyal, U. Das, J. Chem. Res. Synop. 7 (1997) 266.
[10] L. Shen, S. Cao, J. Wu, J. Zhang, H. Li, N. Liu, X. Qian, Green Chem. 11 (2009) 1414–1420.
[11] O. D'Alessandro, A.G. Sathicq, J.E. Sambeth, H.J. Thomas, G.P. Romanelli, Catal. Commun. 60 (2015) 65–69.
[12] N. Koukabi, E. Kolvari, A. Khazaei, M.A. Zolfigol, B. Shirmardi-Shaghasemi, H. Reza Khavasi, Chem. Commun. 47 (2011) 9230–9232.
[13] J.M. Gottfried, Surf. Sci. Rep. 70 (2015) 259–379.
[14] A.B. Sorokin, Chem. Rev. 113 (2013) 8152–8191.
[15] J.L. Heinecke, C. Khin, J.C. Melo Pereira, S.A. Suárez, A.V. Iretskii, F. Doctorovich, P.C. Ford, J. Am. Chem. Soc. 135 (2013) 4007–4017.
[16] S.M. Paradine, M.C. White, J. Am. Chem. Soc. 134 (2012) 2036–2039.
[17] S.Y. Yan, Y. Wang, Y.J. Shu, H.H. Liu, X.G. Zhou, J. Mol. Catal. 248 (2006) 148–151.
[18] S.L. Jain, J.K. Joseph, S. Singhal, B. Sain, J. Mol. Catal. 268 (2007) 134–138.
[19] C. Röhlich, K. Köhler, Adv. Synth. Mater. Catal. 352 (2010) 2263–2274.
[20] J.A. Becerra, L.M. Gonzalez, A.L. Villa, J. Mol. Catal. A 423 (2016) 12–21.
[21] L.M. Gonzalez, A.L. Villa, C. Montes de C, A. Sorokin, Tetrahedron Lett. 47 (2006) 6465–6468.
[22] M.-S. Liao, T. Kar, S.M. Gorun, S. Scheiner, Inorg. Chem. 43 (2004) 7151–7161.
[23] V.H.A. Pinto, J.S. Reboucas, G.M. Ucoski, E.H. de Faria, B.F. Ferreira, R.A. Silva San Gil, S. Nakagaki, Appl. Catal. A 526 (2016) 9–20.
[24] S.V. Sirotin, A.Y. Tolbin, I.F. Moskovskaya, S.S. Abramchuk, L.G. Tomilova, B.V. Romanovsky, J. Mol. Catal. A 319 (2010) 39–45.
[25] S. Rostamnia, E. Doustkhah, RSC Adv. 4 (2014) 28238–28248.
[26] S. Rostamnia, H. Xin, X. Liu, K. Lamei, J. Mol. Catal. A 374–375 (2013) 85–93.
[27] E. Doustkhah, S. Rostamnia, A. Hassankh, J. Porous Mater. 23 (2016) 549–556.
[28] A. Alizadeh, S. Rostamnia, Synthesis 23 (2010) 4057–4060.
[29] S. Rostamnia, K. Lamei, Chin. Chem. Lett. 23 (2012) 930–932.
[30] S. Rostamnia, A. Morsali, RSC Adv. 4 (2014) 10514–10518.
[31] S. Rostamnia, A. Nuri, H. Xin, A. Pourjavadi, S.H. Hosseini, Tetrahedron Lett. 54 (2013) 3344–3347.
[32] S. Das Sharma, P. Hazarika, D. Konwar, Catal. Commun. 9 (2008) 709–714.
[33] M. Filipan-Litvic, M. Litvic, V. Vinkovic, Med. Bioorg. Chem. 16 (2008) 9276–9282.
[34] M. Filipan-Litvic, M. Litvic, V. Vinkovic, Tetrahedron 64 (2008) 5649–5656.
[35] J.H. Weber, D.H. Busch, Inorg. Chem. 4 (1965) 469–471.
[36] S.K. Saini, A. Jena, J. Dey, A.K. Sharma, R. Singh, Magn. Reson. Imaging 13 (1995) 985–990.
[37] A. Hadash, A. Sorokin, A. Rabion, B. Meunier, New J. Chem. 22 (1998) 45–51.
[38] J. Metz, O. Schneider, M. Hanack, Inorg. Chem. 23 (1984) 1065–1071.
[39] P. Shah, A.V. Ramaswamy, K. Lazar, V. Ramaswamy, Appl. Catal. A 273 (2004) 239–248.
[40] Y. Yang, Y. Zhang, S. Hao, J. Guan, H. Ding, F. Shang, P. Qiu, Q. Kan, Appl. Catal. A 381 (2010) 274–281.
[41] A.B. Sorokin, A. Tuel, N. J. Chem. 23 (1999) 473–476.
[42] A.B. Sorokin, A. Tuel, Catal. Today 57 (2000) 45–59.
[43] H. Miyamura, K. Maehata, S. Kobayashi, Chem. Commun. 46 (2010) 8052–8054.
[44] R.E. Parton, P.E. Neys, P.A. Jacobs, R.C. Sosa, P.G. Rouxhet, J. Catal. 164 (1996) 341–346.
[45] B.I. Kharisov, Ingenierías 6 (2003) 3–5.
[46] N. Grootboom, T. Nyokong, J. Mol. Catal. A 179 (2002) 113–123.
[47] M. Vinod, T. Kr Das, A.J. Chandwadkar, K. Vijayamohanan, J.G. Chandwakar, Mater. Chem. Phys. 58 (1999) 37–41.
[48] S. Seelan, A.K. Sinha, Appl. Catal. A 238 (2003) 201–209.
[49] M.A. Zanjanchi, K. Tabatabaeian, M. Moosavifar, J. Incl. Phenom. Macrocycl. Chem. 40 (2001) 193–198.
[50] R. Seudi, G.S. El-Bahy, Z. Sayed, Opt. Mater. 29 (2006) 304–312.
[51] M.M. El-Nahass, K.F. Abd-El-Rahman, A. Darwish, Mater. Chem. Phys. 92 (2005) 185–189.
[52] Pretsch, Clerc, Seibl, Simon, Tables of Spectral Data for Structure Determination of Organic Compounds. 13C NMR, 1H NMR, IR, MS, UV/VIS, 2nd edition, Springer Verlag, 1999.
[53] Z. Liu, X. Zhang, Y. Zhang, J. Jiang, Spectrochim. Acta Part A 67 (2007) 1232–1246.
[54] J. Jiang, M. Bao, L. Rintoul, D.P. Arnold, Coord. Chem. Rev. 250 (2006) 424–448.
[55] F. Lu, W. Wang, G. Bao, J. Cui, Vib. Spectrosc. 56 (2011) 228–234.
[56] G. Bao, W. Wang, Y. Mao, F. Lu, Spectrochim. Acta Mol. Biomol. Spectrosc. 102 (2013) 275–280.
[57] K. De Wael, P. Westbroek, P. Bultinck, D. Depla, P. Vandenabeele, A. Adriaens, E. Temmerman, Electrochem. Commun. 7 (2005) 87–96.
[58] B. Tatar, D. Demiroğlu, Mater. Sci. Semicond. Process. 31 (2015) 644–650.
[59] J.B. Lambert, H.F. Shurvell, R.G. Cooks, Introduction to Organic Spectroscopy, 1st ed., Macmillan, 1987.
[60] S. Ko, M.N.V. Sastry, C. Lin, C.F. Yao, Tetrahedron Lett. 46 (2005) 5771–5774.
[61] F. Arena, R. Dario, A. Parmaliana, Appl. Catal. A 170 (1998) 127–137.
[62] L.M. González, Monoterpenes oxyfunctionalization, Universidad de Antioquia, 2008, doctoral thesis.
[63] C. Isvoranu, B. Wang, E. Ataman, K. Schulte, J. Knudsen, J.N. Andersen, M.L. Bocquet, J. Schnadt, J. Chem. Phys. 134 (2011), 114710-1–114710-10.
[64] J. Yan, C. Zhang, C. Ning, Y. Tang, Y. Zhang, L. Chen, S. Gao, Z. Wang, W. Zhang, J. Ind. Eng. Chem. 25 (2015) 344–351.
[65] Y. Chen, Y. Cao, Y. Suo, G.P. Zheng, X.X. Guan, X.C. Zheng, J. Taiwan Inst. Chem. Eng. 51 (2015) 186–192.
[66] Y. Shao, K. Zhu, Z. Qin, E. Li, Y. Li, J. Org. Chem. 78 (2013) 5731–5736.
[67] A. Shaabani, S. Keshipour, M. Hamidzad, S. Shaabani, J. Mol. Catal. A 395 (2014) 494–499.
[68] X. Jia, L. Yu, C. Huo, Y. Wang, J. Liu, X. Wang, Tetrahedron Lett. 55 (2014) 264–266.
[69] A.L. Villa, L.M. Sánchez, H.J. Thomas, G.P. Romanelli, L.M. Gonzalez, Memorias VIII Simposio Colombiano de Catálisis, 2013, Armenia-Colombia.
[70] M.M. Heravi, H.A. Oskooie, R. Malakooti, B. Alimadadi, H. Alinejad, F.K. Behbahani, Catal. Commun. 10 (2009) 819–822.
[71] M.E. Ortiz, L.J. Núñez-Vergara, C. Camargo, J.A. Squella, Pharm. Res. 21 (2004) 428–435.